Chaotic and regular behavior of a trapped ion interacting with a laser field

R. Chacón and J. I. Cirac
Departamento de Fisica Aplicada, Universidad de Catilla—La Mancha, Campus Universitario, 13071 Ciudad Real, Spain
(Received 7 October 1994)

We study analytically and numerically the motion of a trapped two-level ion in the presence of a resonant laser field. Using a semiclassical description, we find that for sufficiently strong laser fields atomic motion becomes chaotic for a wide range of parameters and initial conditions. The traces of chaotic motion are reflected in the population inversion of the trapped ion, and thus could be observed by using the quantum jump technique.

PACS number(s): 32.80.Pj, 42.50.Vk, 05.45.+b

I. INTRODUCTION

The interaction between a single trapped ion and a laser field has become a problem of increasing interest during the last few years, especially in the field of quantum optics and precision spectroscopy. Of particular interest is the situation in which the laser field is quasiresonant with a metastable transition of the trapped ion. From an experimental point of view, dipole-forbidden transitions have been used to cool an Hg^+ ion to very low temperatures via sideband cooling [1] and to measure the temperature of the ion using the quantum jump technique [2]. From a theoretical point of view, dissipation in the system is negligible which leads to a number of interesting phenomena [3–5].

Most of the theoretical analysis of the interaction between laser fields and ions without dissipation is based on two approximations: (i) the so-called Lamb-Dicke limit and (ii) the secular approximation. In the Lamb-Dicke limit, the motion of the ion is restricted to a region that is small as compared to the laser wavelength, which introduces important simplifications in the problem [6,7]. The secular approximation is related to the fact that for ions confined in a Paul trap one usually replaces the time-dependent trapping potential by a harmonic potential. This amounts to averaging the atomic motion during small time intervals, and therefore neglecting the rapid oscillations (micromotion) of the ion in front of its slow motion (secular motion). In fact, in the Lamb-Dicke limit and for laser frequencies not too far off the atomic resonance this last assumption is very well satisfied in the context of laser cooling [8]. Under these approximations, the problem of the motion of a two-level ion interacting with laser light (without dissipation) is very similar to that found in cavity QED, where instead of the motion of the ion in a harmonic potential one has a single mode (cavity mode) of the radiation field. Using this similarity, one can prepare nonclassical states of motion of the ion [4], as well as observe the collapse and revival of its population inversion [3]. However, in situations where the Lamb-Dicke limit is not satisfied, all these phenomena are expected to be modified. In particular, the micromotion of an ion in a Paul trap can become important and lead to other phenomena not considered so far. It is thus clear that a full description of this problem, including the micromotion of the ion in the trap, would be desirable.

In this paper we analyze the interaction of a two-level ion in a Paul trap with a laser field on resonance with the two-level transition. We employ a semiclassical description, whereby the motion of the ion is treated classically. Furthermore, we consider the laser field in a standing-wave configuration, since this notably simplifies the problem. We expect, however, the same qualitative behavior for laser fields in traveling-wave configurations. We will show that under certain conditions the motion of the ion is chaotic. Essentially, this occurs when the energy due to the laser-induced potential (a sine function) is comparable to that of the trapping potential, and for initial conditions rather close to the separatrix of the time-independent problem. The ion, in this case, tends to jump from one of the induced wells to another in an stochastic way. We use the Melnikov analysis [9] to determine the range of physical parameters which leads to instability and chaotic motion. We also characterize the regular and chaotic motion by usual methods: the Lyapunov characteristic exponent and the power spectrum. We explain qualitatively the numerical results through analytical expressions derived when micromotion is neglected. In such a case, the problem is exactly solvable and therefore no chaotic motion occurs. We note that a full quantum treatment of the motion of an ion in a Paul trap, in the absence of any laser field, has been given in Refs. [14,15]. On the other hand, laser cooling in the Lamb-Dicke limit including micromotion has been studied in Refs. [8,16].

Recently observed dynamical effects with a small number of laser-cooled trapped ions suggest the occurrence of (classical) chaos in ion dynamics [10]. For this system, chaos has been attributed to the nonlinearity arising from the ion-ion Coulomb repulsion [11], rather than to the ion-trap system. Thus the existence of chaos in ion traps has been connected so far to the presence of two or more ions in the trap [12,11,13]. So, for those studies, the secular approximation is taken when considering the action of the trapping potential. We wish to stress the fact that the existence of chaos in ion traps has been connected so far to the presence of two or more ions in the trap. As we show in this paper, chaos can also occur with a single ion

1050-2947/95/51(6)/4900(6)/$06.00

in the trap. Recent advances in laser cooling and trapping of single ions in traps could lead to an experimental observation of this phenomenon in the near future.

This paper is organized as follows. In Sec. II we introduce the model and derive the evolution equations for the motion of the ion. In Sec. III we derive analytical results under certain limits. In Sec. IV we derive an expression for the Melnikov function, which determines the "degree of chaos" for a given set of parameters. A discussion of the numerical results is given in Sec. V. Finally, Sec. VI includes a summary of the results.

II. MODEL

We consider a single two-level ion trapped in a Paul trap. The ion interacts with a resonant laser standing wave, propagating along the x direction. The Hamiltonian describing this situation in a rotating frame at the laser frequency is ($\hbar = 1$)

$$H = \frac{\vec{p}^{\,2}}{2m} + U(\vec{r}, t) + \frac{\Omega_0}{2}\sigma_x \sin(kx + \phi). \tag{1}$$

Here, $\vec{r}$ and $\vec{p}$ denote the position and momentum of the ion (center of mass), m is the ion mass, σ_x is a spin-$\frac{1}{2}$ operator for the two-level system, Ω_0 (> 0) is the Rabi frequency for the laser-ion interaction, and ϕ gives the relative position between the center of the Paul trap and the laser standing wave. $U(\vec{r}, t)$ is the trapping potential and is given by

$$U(\vec{r}, t) = \frac{1}{2} m W(t)(x^2 + y^2 - 2z^2), \tag{2}$$

where

$$W(t) = \frac{\omega^2}{4}[a - 2q\cos(\omega t)], \tag{3}$$

with ω being the micromotion frequency, and a and q depending on the specific geometry and applied voltages to the trap. Note that the motions in the x, y, and z directions are completely decoupled. This is due to the fact that the laser field only modifies the motion in the x direction through the photon recoil accompanying each absorption and emission of laser photons. Thus the motion in the y and z directions does not depend on the laser field, so that y and z fulfill Mathieu equations and therefore they present regular behavior. Consequently, we will restrict ourselves to the one-dimensional problem of the motion of the ion along the x direction.

Starting from the Hamiltonian (1) one can easily derive the equations describing the evolution of the ion. In particular, the equations for the *internal dynamics* are the following:

$$\dot{\sigma}_x = 0, \tag{4a}$$

$$\dot{\sigma}_y = -\Omega_0 \sin(kx + \phi)\sigma_z, \tag{4b}$$

$$\dot{\sigma}_z = \Omega_0 \sin(kx + \phi)\sigma_y, \tag{4c}$$

where the sigmas are spin-$\frac{1}{2}$ operators describing the two-level system. These are the familiar Bloch equations (in the absence of dissipation), where now the effective Rabi frequency depends on the specific location of the ion x. From these equations one has that σ_x is a constant of motion. Taking as the initial state of the two-level system [17]

$$\frac{1}{\sqrt{2}}(|g\rangle + e^{-i\theta}|e\rangle), \tag{5}$$

where $|g\rangle$ and $|e\rangle$ denote the ground and excited state, respectively, we have that $\langle\sigma_x\rangle = \cos(\theta)$. On the other hand, one can easily solve the equations for σ_y and σ_z in terms of $x(t)$, obtaining

$$\langle\sigma_y(t)\rangle = \sin(\theta)\cos\left[\Omega_0 \int_0^t \sin[kx(t') + \phi]dt'\right], \tag{6a}$$

$$\langle\sigma_z(t)\rangle = \sin(\theta)\sin\left[\Omega_0 \int_0^t \sin[kx(t') + \phi]dt'\right]. \tag{6b}$$

Equations (6) show that a chaotic motion gives rise to chaotic dynamics for both σ_y and σ_z. This fact provides a method to detect chaos in the motion, since in ion traps one can easily measure σ_z by the quantum jumps technique [2].

For the equations describing the *external dynamics* (center-of-mass motion) we have

$$\ddot{x} = -W(t)x - \frac{\Omega_0 k}{2m}\cos(\theta)\cos(kx + \phi). \tag{7}$$

Defining new variables,

$$\tilde{x} = kx, \tag{8a}$$

$$\tau = \omega t/2, \tag{8b}$$

we have

$$\tilde{x}'' = -f(\tau)\tilde{x} - \Omega\cos(\tilde{x} + \phi), \tag{9}$$

where $f(\tau) = a - 2q\cos(2\tau)$, and

$$\Omega = \frac{2k^2\Omega_0\cos(\theta)}{m\omega^2} \equiv 4\cos(\theta)\eta^2\frac{\Omega_0}{\omega}. \tag{10}$$

With these definitions we reduce the number of parameters involved in the problem to four dimensionless parameters: a, q, ϕ, and Ω. Note that Ω is proportional to the Rabi frequency Ω_0, the energy recoil $k^2/(2m)$, and is inversely proportional to the square of the micromotion frequency ω. This combination of parameters in Ω, together with the specific characteristics of the trap (a and q) determine the motion of the ion. In the limit $\Omega \to 0$, Eq. (9) reduces to the Mathieu equation [18], whereas for $a, q \to 0$ (or, equivalently, $\Omega \to \infty$) one recovers the pendulum equation. On the other hand, the solution to Eq. (9) determines completely the evolution of both the external and internal dynamics [cf. Eq. (6)].

III. ANALYTICAL APPROXIMATIONS

A. Secular motion

This approximation is based on the substitution of the time-dependent trapping potential by a simple harmonic oscillator. This amounts to neglecting the micromotion. The secular frequency that characterizes the trap is

$$\nu = \frac{\omega}{2}\sqrt{a + q^2/2}. \qquad (11)$$

Under this approximation, the Hamiltonian for the one-dimensional (1D) problem becomes

$$H = \frac{p^2}{2m} + \frac{1}{2}m\nu^2 x^2 + \frac{\Omega_0}{2}\sigma_x \sin(kx + \phi), \qquad (12)$$

which, obviously, is integrable. The motion of the ion depends on the relative strengths between the harmonic oscillator and the laser-induced potential. For example, for $\phi = 3\pi/2$ (the minima of both potentials coincide at $x = 0$), we have that when $4\nu^2/\omega^2 \gg \Omega$ it is the harmonic potential the one that influences the motion of the ion, whereas in the opposite limit, the laser interaction dominates.

In principle, one may expect [8] that the Hamiltonian (12) provides a good approximation to the (time-averaged) dynamics for $\nu \ll \omega$ (or, equivalently, $a, q \ll 1$). However, this is not always the case as will be proved in the next section. There we show that even for $a = 0$ and q small, the atomic motion can become chaotic, for a given set of initial conditions. On the contrary, in the case of regular motion Hamiltonian (12) provides with a very good description of the dynamics.

B. Lamb-Dicke limit

In the Lamb-Dicke limit, the ion oscillates in a region which is much smaller than the laser wavelength. In this case, $|\tilde{x} - \tilde{x}_0| \ll 1, \forall\tau$, where $\tilde{x}_0$ is the position around where the ion oscillates. This limit allows us to expand the equations of Sec. II in powers of $(\tilde{x} - \tilde{x}_0)$, keeping the lowest orders. The resulting evolution equation for $\tilde{x}$ becomes [18]

$$\tilde{x}'' = -\tilde{f}(\tau)\tilde{x} + C, \qquad (13)$$

where $\tilde{f}$ is the same as f but with the replacement

$$a \to a_{eff} = a - \Omega \sin(\tilde{x}_0 + \phi), \qquad (14)$$

and $C = \Omega[\cos(\tilde{x}_0 + \phi) - \tilde{x}_0 \sin(\tilde{x}_0 + \phi)]$ is a constant. Let us analyze the simplest case when $x_0 = 0$ and $\phi = 3\pi/2$. Then, (13) reduces to the familiar Mathieu equation [18]. This fact allows us to predict whether the motion of the ion will be bounded or not. According to [18], the first stable region of the Mathieu equations (which is the one currently used in most experiments dealing with Paul traps [3]) is bounded by the curves

$$a_0(q) = -\frac{q^2}{2} + \frac{7q^4}{128} + \cdots, \qquad (15a)$$

$$b_1(q) = 1 - q - \frac{q^2}{8} + \frac{q^3}{64} - \frac{q^4}{1536} + \cdots. \qquad (15b)$$

For $\Omega = 0$ (i.e., in the absence of the laser field), stable motion occurs for values of a and q with $a_0(q) \le a \le b_1(q)$ [19]. Increasing the laser intensity leads to a modification of the effective parameter a_{eff}. Then, for sufficiently high laser power, the ion parameter cross one of the borders (15) and its motion becomes unbounded. This occurs when either $a_0(q) = a_{eff}$ or $b_1(q) = a_{eff}$. In summary, under Lamb-Dicke limit conditions, for high laser intensities the stable motion can disappear. This statement agrees with the results derived in the next section. Note that although Eq. (13) does not predict chaos, this is not necessarily the case. This is due to the fact that when the parameters q and a_{eff} lie out of the stable region, the Lamb-Dicke limit is not longer valid, nor is Eq. (13).

IV. MELNIKOV ANALYSIS

In the absence of micromotion ($a = q = 0$) the evolution equation of the motion is that of a simple pendulum. The main effect of micromotion ($q \neq 0$) is to yield, under appropriate conditions, a homoclinic bifurcation in (9). This leads to the appearance of an unstable layer — meaning the possibility of stochastic motion— along the separatrix of the unperturbed pendulum. If the strength of micromotion remained constant in time, this exceedingly complicated behavior should occur in a region of the phase space bounded between Kolmogorov-Arnold-Moser (KAM) curves. On the contrary, the multiplicative nature of the perturbation may render the overall perturbation relatively large and, as a consequence, the orbits can chaotically escape from the initial well, as observed in numerical experiments. In this section we use the Melnikov method [9,20,21] to determine under what conditions a homoclinic bifurcation occurs in (9), and for calculating the width of the stochastic layer. This last term is used to denote the region in phase space where the motion becomes irregular.

We now briefly describe this method for the particular case of a Hamiltonian system, with one degree of freedom, subjected to a Hamiltonian perturbation [21]. Consider a system described by the following equations:

$$\dot{\mathbf{x}} = \mathbf{h}_0(\mathbf{x}) + \epsilon\mathbf{h}_1(\mathbf{x}, t), \qquad (16a)$$

$$\mathbf{x} = (x, v), \qquad (16b)$$

where the unperturbed equation ($\epsilon = 0$) comes from an integrable Hamiltonian system with a hyperbolic fixed point P_0, a separatrix orbit $x_0(t)$ [such that $\lim_{t\to\pm\infty} x_0(t) = P_0$], and $\mathbf{h}_1$ is a function of time with period T. Due to this nonautonomous forcing, the irregular motion will occur for orbits whose initial conditions are near the separatrix $x_0(t)$. Melnikov [9] introduced a simple function $\Delta(t_0)$ that, when it has a simple zero (for some t_0), indicates the presenence of stochastic motion. The width d of the stochastic layer can be estimated from the Melnikov function as [20,21]

$$d = \left|\left| \frac{\epsilon\Delta(t_0)}{|\mathbf{h}_0[x_0(0)]|} \right|\right|_{\max t_0} + O(\epsilon^2). \qquad (17)$$

In order to apply the method described above to Eq. (9) we rewrite it in first-order form

$$\tilde{x}' = \tilde{v}, \tag{18a}$$

$$\tilde{v}' = 2q\left[\tilde{x} + \frac{\pi}{2} - \phi\right]\cos(2\tau) - \Omega\sin(\tilde{x}), \tag{18b}$$

where, for the sake of simplicity, we assumed $a = 0$, $0 < \theta < \frac{\pi}{2}$ (i.e., $\Omega > 0$), and we applied the substitution $\tilde{x} \to \tilde{x} - \phi - \pi/2$ to Eq. (9). Also, we take the limit $0 < q \ll 1$. For $q = 0$, as mentioned above, one recovers the integrable pendulum with separatrix,

$$\tilde{x}_0(\tau) = \pm 2\arctan[\sinh(\sqrt{\Omega}\,\tau)], \tag{19a}$$

$$\tilde{v}_0(\tau) = \pm 2\sqrt{\Omega}\,\mathrm{sech}(\sqrt{\Omega}\tau), \tag{19b}$$

where the positive (negative) sign refers to the top (bottom) homoclinic orbit. Under micromotion perturbation, $0 < q \ll 1$, we consider the extended phase space $(\tilde{x}, \tilde{v}, \tau)$. In particular, we examine the Poincare section $t = \text{const} \pmod{\pi}$. To compute the width of the stochastic layer, we calculate the Melnikov function:

$$\Delta^{\pm}(t_0) = 2q\left[\int_{-\infty}^{\infty} \tilde{x}_0(t)\tilde{v}_0(t)\cos[2(\tau+t_0)]d\tau + \left(\frac{\pi}{2} - \phi\right)\int_{-\infty}^{\infty} \tilde{v}_0(t)\cos[2(\tau+t_0)]d\tau\right], \tag{20}$$

which measures the distance between the stable and unstable orbits in the Poincare section at t_0. Substituting (19) into (20), and after some algebraic manipulation, we obtain

$$\Delta^{\pm}(t_0) = 4q\left(4R(\Omega)\sin(2t_0) \pm \pi\left[\frac{\pi}{2} - \phi\right]\mathrm{sech}\left[\frac{\pi}{\sqrt{\Omega}}\right]\cos(2t_0)\right), \tag{21}$$

with

$$R(\Omega) \equiv \int_0^{\infty} \arctan[\sinh(\tau)]\mathrm{sech}(\tau)\sin\left[\frac{2\tau}{\sqrt{\Omega}}\right]d\tau. \tag{22}$$

It is straightforward to show that $R(\Omega)$ is positive; it tends to zero for $\Omega \to 0, \infty$ and has a maximum at about $\Omega \simeq 1$. Thus it is clear that $\Delta^{\pm}(t_0)$ has simple zeros, indicating the existence of stochastic behavior for orbits whose initial conditions are sufficiently near the unperturbed separatrix (19). Using Eq. (17), the width of the stochastic layer is given by

$$d(q,\Omega,\phi) = 16q\left[\Omega^{-1}\left(R(\Omega)^2 + \left[\frac{\pi}{4}\right]^2\left[\phi - \frac{\pi}{2}\right]^2\mathrm{sech}^2\left[\frac{\pi}{\sqrt{\Omega}}\right]\right)\right]^{1/2} + O(q^2). \tag{23}$$

It is expected that almost all orbits starting in some point inside the layer be chaotic. A more delicate question is how large we can make q for our above results to be valid (notice that the Melnikov method, being based on perturbation theory, is approximate). For the micromotion term the perturbative requirement is written as $|2q(\tilde{x} - \phi + \pi/2)| \ll 1$. Then the upper threshold is obtained for motions that stay close to the separatrix:

$$q \ll q_{th}(\phi) \equiv \frac{1}{2|3\pi/2 - \phi|}. \tag{24}$$

Note that, for fixed values of q and Ω, the function $d(\phi)$ [see Eq. (23)] presents a minimum at $\phi = \pi/2$. This value corresponds with the physical situation where the harmonic secular potential is centered at the node of the standing wave, so that both minima (from the laser-induced potential and the harmonic one) coincide. It is not surprising that the "most stable" situation corresponds to these parameters, since the action of the laser adds up to that of the trapping potential to confine the ion in a specific region of the space.

On the other hand, from Eqs. (22) and (23) we obtain the following limits, for fixed values of q and ϕ:

$$\lim_{\Omega \to 0,\infty} d(q,\Omega,\phi) = 0. \tag{25}$$

Thus in these limits chaotic motion is not possible. These limits were discussed at the end of Sec. II.

V. NUMERICAL RESULTS

We have performed some computer simulations on the system described by Eq. (9). A systematic numerical survey of its parameter space is beyond our aim. Therefore, we have chosen some arbitrary sets of parameters in order to illustrate the predictions of the Melnikov method. In particular, with a fixed set of parameters (q, Ω, ϕ), we study the orbits based on different initial conditions with increasing proximity to the unperturbed separatrix. Regular and stochastic motions were detected by standard methods: the Lyapunov exponent and power spectrum. The Lyapunov exponent [21,22] is given by

$$\lambda = \lim_{t\to\infty} \frac{1}{t}\mathrm{Ln}\frac{||\mathbf{W(t)}||}{||\mathbf{W}(0)||}, \tag{26}$$

where $\mathbf{W}(t)$ represents the tangent vector associated with a given reference orbit governed by the system which we denote $d\mathbf{x}/dt = \mathbf{F}(\mathbf{x}(t))$. Thus $\mathbf{W}(t)$ is governed by the equation $d\mathbf{W}(t)/dt = \mathbf{M}(\mathbf{x}(t))\mathbf{W}(t)$, where $\mathbf{M}$ is the Jacobean matrix associated with $\mathbf{F}$. The computation of Lyapunov exponents is a standard tool for measuring stochastic properties of Hamiltonian systems [21]. A Hamiltonian system with n degrees of freedom has $2n$ Lyapunov exponents associated with a given reference orbit. These exponents verify the symmetry property $\lambda_i = -\lambda_{2n-i+1}$ for $1 \le i \le 2n$. Moreover, a given orbit always has one exponent which is zero. Thus for our case $n = 1.5$, there is at most one positive exponent for any given reference orbit.

We compute the Lyapunov exponents by using a version of the algorithm introduced in Ref. [22] and used in Ref. [23]. As integrator we have adopted a Bulirsch-Stoer routine [24]. In taking the limit required by (26) we typi-

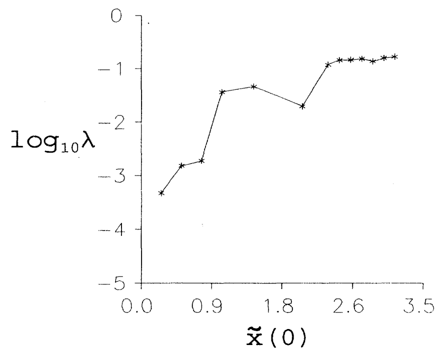

FIG. 1. $\mathrm{Log}_{10}(\lambda)$ versus $\tilde{x}(0)$ for $\tilde{v}(0) = 0$, $\phi = \pi/2$, $q = 0.05$, and $\Omega = 1.5462$.

cally integrate up to $t = 30\,000$ which is sufficient for our purposes.

Figure 1 shows a plot of $\log_{10}(\lambda)$ as a function of the displacement $\tilde{x}(0)$ (λ the positive Lyapunov exponent) for the set of parameters $\{\tilde{v}(0), \phi, q, \Omega\} = \{0, \pi/2, 0.05, 1.5462\}$. The values for λ fluctuate, but with an overall increasing trend as the top of the well is approached. In Fig. 2 we plot $\log_{10}(\lambda)$ versus $\log_{10}(t)$ for two cases, showing the convergence of λ as $t \to \infty$. Figure 2(a) corresponds to $\tilde{x}(0) = 2.87$ while 3(b) corresponds to $\tilde{x}(0) = 0.25$. The final values of λ for these cases are roughly 0.1387 and 0.0005, respectively. From Eq. (23) the theoretical width of the stochastic layer is $d(0.05, 1.5462, \pi/2) = 0.2704$, i.e., it is smaller than the one observed numerically. But this result is not surprising since the Melnikov method, which is based on the perturbation theory, is approximate. Similar discrepancies between these types of analytical and numerical predictions were found in other contexts [25].

Generally, small values of the positive Lyapunov exponent (typically, $\lambda \lesssim 10^{-3}$) correspond to stochastic motions confined in the well for long periods, whereas higher values mean that the ion jumps quickly to another well in a chaotic way. Another way of detecting the same phenomenon is by looking at the spectral prop-

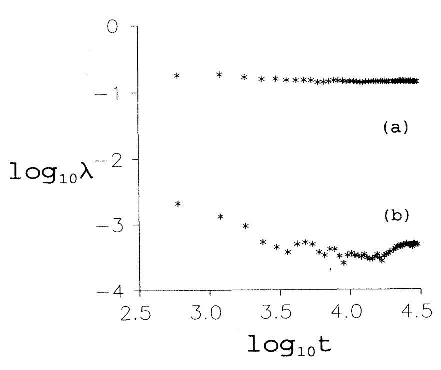

FIG. 2. $\mathrm{Log}_{10}(\lambda)$ versus $\log_{10}(t)$ for two different initial conditions, the remaining parameters being the same as in Fig. 1. (a) $\tilde{x}(0) = 2.87$; (b) $\tilde{x}(0) = 0.25$.

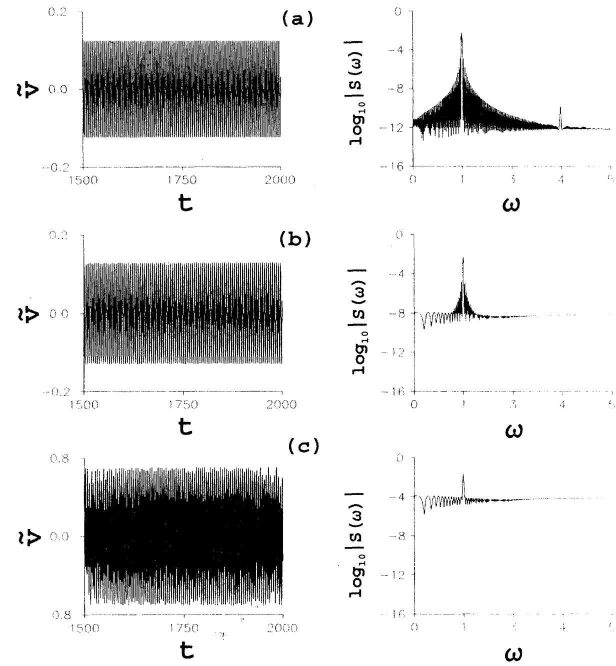

FIG. 3. Time series of the velocity and corresponding power spectra for $\tilde{x}(0) = 0.1$, $\tilde{v}(0) = 0$, $\phi = \pi/2$, and $\Omega = 1.5462$. (a) $q = 10^{-5}$, periodic motion. (b) $q = 10^{-3}$, beginning of the amplitude fluctuations. (c) $q = 10^{-1}$, the random amplitude fluctuations are clearly visible.

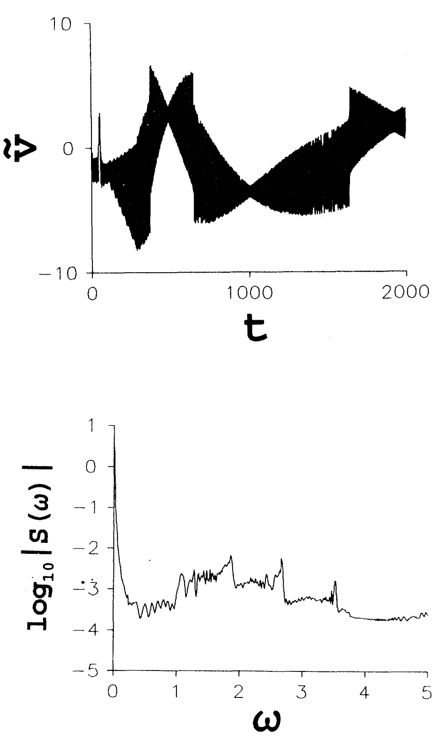

FIG. 4. Same as in Fig. 3 with $\tilde{x}(0) = 2.6$, $\tilde{v}(0) = 0$, $\phi = \pi/2$, and $\Omega = 1.5462$. (a) $q = 0.05$.

erties of the solutions. From numerical integration one obtains pseudo-orbits of the system in the form of the time series $f(t)$; then, standard fast-Fourier transform yields the power spectrum $S(\omega) = |a(\omega)|^2$. Usual averaging procedures have been used to improve its quality [24].

In Fig. 3 we plot three time series of the velocity, and their corresponding power spectra, for increasing values of q. Comparison among Figs. 3(a)–3(c) clearly shows that when q increases, the periodic component (at $\omega = \sqrt{\Omega}$) of the spectrum is reduced and its random component is magnified. Observe that the case shown in Fig. 3(c) indicates chaotic dynamics limited to the original well, and therefore this regime could be more easily detected experimentally. Finally, in Fig. 4, we give an example of stochastic escape. The time series of the velocity [Fig. 4(a)] is very irregular and the associated power spectrum [Fig. 4(b)] contains substantial power at low frequencies.

VI. SUMMARY

We have studied the motion of a single ion, trapped in a Paul trap, and interacting with a resonant laser beam in standing-wave configuration. We have used a semiclassical approximation, whereby the motion of the ion is treated classically, whereas its internal dynamics is described quantum mechanically. We have studied the regimes characterized by secular motion and the Lamb-Dicke limit. The analysis performed using the Melnikov method predicts the existence of chaotic behavior for initial conditions close to the separatrix of the pendulum case ($a = q = 0$). We have derived an analytical expression for the width of the stochastic layer around such a separatrix. Numerical results confirm the existence of chaos in this problem. We have characterized the chaos by using the Lyapunov exponent and the power spectrum. The traces of the chaotic motion could be measured in an ion trap by detecting the internal state of the ion as a function of time, since the population inversion also displays chaotic behavior. We expect that a thorough extension of the present work to the case where the motion of the ion is treated quantum mechanically will reveal other interesting behavior. In particular, this could serve as a simple model to study quantum chaos.

ACKNOWLEDGMENTS

J.I. Cirac acknowledges fruitful discussions with R. Blatt and P. Zoller.

[1] F. Diedrich, J.C. Berquist, W.M. Itano, and D.J. Wineland, Phys. Rev. Lett. **62**, 403 (1989).
[2] W. Nagourney, J. Sandberg, and H. Dehmelt, Phys. Rev. Lett. **56**, 2797 (1986); T. Sauter, W. Neuhauser, R. Blatt, and P.E. Toschek, *ibid.* **57**, 1696 (1986); J.C. Bergquist *et al.*, *ibid.* **57**, 1699 (1986).
[3] C.A. Blockley, D.F. Walls, and H. Risken, Europhys. Lett. **17**, 509 (1992); J.I. Cirac, R. Blatt, A.S. Parkins, and P. Zoller, Phys. Rev. A **49**, 1202 (1993).
[4] J.I. Cirac, R. Blatt, A.S. Parkins, and P. Zoller, Phys. Rev. Lett. **70**, 556 (1994); **70**, 762 (1994); J.I. Cirac, R. Blatt, and P. Zoller, Phys. Rev. A **49**, R3174 (1994).
[5] R. Blatt, J.I. Cirac, A.S. Parkins, and P. Zoller, Phys. Scr. (to be published).
[6] See, for example, S. Stenholm, Rev. Mod. Phys. **58**, 699 (1986).
[7] See, for example, J. Mod. Opt. **39**, 192 (1992), special issue on the physics of trapped ions, edited by R. Blatt, P. Gill, and R.C. Thompson.
[8] J.I. Cirac, L.J. Garay, R. Blatt, A.S. Parkins, and P. Zoller, Phys. Rev. A **49**, 421 (1994).
[9] V.K. Melnikov, Trans. Moscow Math. Soc. **12**, 1 (1963).
[10] J. Hoffnagle, R.G. DeVoe, L. Reyna, and R.G. Brewer, Phys. Rev. Lett. **61**, 255 (1988).
[11] R.G. Brewer, J. Hoffnagle, R.G. DeVoe, L. Reyna, and W. Henshaw, Nature **344**, 305 (1990).
[12] R. Blümel, C. Kappler, W. Quint, and H. Walther, Phys. Rev. A **40**, 808 (1989).
[13] G. Baumann and T.F. Nonnenmacher, Phys. Rev. A **46**, 2682 (1992).
[14] R.J. Glauber, in *Foundations of Quantum Mechanics*, edited by T.D. Black, M.M. Nieto, H.S. Pilloff, M.O. Scully, and R.M. Sinclair (World Scientific, Singapore, 1992), p. 23.
[15] S. Stenholm, J. Mod. Opt. **39**, 192 (1992).
[16] D.J. Wineland, W.M. Itano, J.C. Bergquist, and R.G. Hulet, Phys. Rev. A **36**, 2220 (1987).
[17] We chose an initial state with $\langle\sigma_x(0)\rangle \neq 0$ since otherwise the effect of the laser on the atomic motion cancels out.
[18] *Handbook of Mathematical Functions*, edited by M. Abramowitz and I.A. Stegun (Dover, New York, 1964).
[19] For a stable motion in all three dimensions one has to consider also the stability conditions for the motion in z, which is different due to the factor -2 in Eq. (2).
[20] J. Guckenheimer and P. Holmes, *Nonlinear Oscillators, Dynamical Systems, and Bifurcations of Vector Fields*, Applied Mathematical Science Vol. 42 (Springer-Verlag, New York, 1983).
[21] A.J. Lichtenberg and M.A. Lieberman, in *Regular and Stochastic Motion*, Applied Mathematical Science Vol. 38 (Springer-Verlag, New York, 1983).
[22] G. Benettin, L. Galgani, and J.M. Streleyn, Phys. Rev. A **14**, 2338 (1976).
[23] A. Wolf, J. Swift, H.L. Swinney, and J. Vastano, Physica **16D**, 285 (1985).
[24] W.M. Press, B.P. Flannery, S.A. Teukolsky, and W.T. Vetterling, *Numerical Recipes: The Art of Scientific Computing* (Cambridge University Press, Cambridge, 1986).
[25] F. Cuadros and R. Chacon, Phys. Rev. E **47**, 4628 (1993).